AAC Journals.ASM.org

Mechanism of Amphotericin B Resistance in Clinical Isolates of *Leishmania donovani*

Bidyut Purkait,[a] Ashish Kumar,[a] Nilay Nandi,[c] Abul Hasan Sardar,[a] Sushmita Das,[a] Sudeep Kumar,[d] Krishna Pandey,[b] Vidyananda Ravidas,[b] Manish Kumar,[a] Tripti De,[e] Dharmendra Singh,[a] and Pradeep Das[a]

Department of Molecular Biology[a] and Department of Clinical Medicine,[b] Rajendra Memorial Research Institute of Medical Sciences, Agamkuan, Patna, Bihar, India; UT Southwestern Medical Center, Dallas, Texas, USA[c]; Institute of Global Health, Internal Medicine, University of New Mexico, Albuquerque, New Mexico, USA[d]; and Indian Institute of Chemical Biology, Kolkata, India[e]

The clinical value of amphotericin B, the mainstay therapy for visceral leishmaniasis in sodium antimony gluconate-nonresponsive zones of Bihar, India, is now threatened by the emergence of acquired drug resistance, and a comprehensive understanding of the underlying mechanisms is the need of the hour. We have selected an amphotericin B-resistant clinical isolate which demonstrated 8-fold-higher 50% lethal doses (LD_{50}) than an amphotericin B-sensitive strain to explore the mechanism of amphotericin B resistance. Fluorimetric analysis demonstrated lower anisotropy in the motion of the diphenylhexatriene fluorescent probe in the resistant strain, which indicated a higher fluidity of the membrane for the resistant strain than for the sensitive strain. The expression patterns of the two transcripts of *S*-adenosyl-L-methionine:C-24-Δ-sterol methyltransferase and the absence of ergosterol, replaced by cholesta-5,7,24-trien-3β-ol in the membrane of the resistant parasite, indicate a decreased amphotericin B affinity, which is evidenced by decreased amphotericin B uptake. The expression level of MDR1 is found to be higher in the resistant strain, suggesting a higher rate of efflux of amphotericin B. The resistant parasite also possesses an upregulated tryparedoxin cascade and a more-reduced intracellular thiol level, which helps in better scavenging of reactive oxygen species produced by amphotericin B. The resistance to amphotericin B was partially reverted by the thiol metabolic pathway and ABC transporter inhibitors. Thus, it can be concluded that altered membrane composition, ATP-binding cassette transporters, and an upregulated thiol metabolic pathway have a role in conferring amphotericin B resistance in clinical isolates of *Leishmania donovani*.

Leishmaniasis, or kala azar, is a group of diseases caused by a protozoan parasite of the genus *Leishmania*. Kala azar is a symptomatic infection of liver, spleen, and bone marrow. The global estimates for the incidence and prevalence of kala azar cases per year are 0.5 and 2.5 million, respectively (57). In India, visceral leishmaniasis (VL) has been reported in parts of West Bengal, Uttar Pradesh, and Bihar. It poses a major health problem in the state of Bihar, which accounts for nearly 90% of the total cases in India (51). Chemotherapy has proven to be the only effective way of controlling infections and is highly dependent upon antimony-containing drugs, such as sodium stibogluconate (Pentostam). Amphotericin B (AmB) is used as the drug of choice when acquired drug resistance emerges for traditional antimony therapy, and nearly 64% of cases in regions of Bihar where VL is hyperendemic are now resistant to antimonials (28). Hexadecylphosphocholine (miltefosine) is the first orally administered drug for VL and the latest to enter the market. The dosing scheme of hexadecylphosphocholine is 100 mg/kg of body weight/day for 28 days in adults weighing ≥50 kg, 50 mg/kg/day in adults weighing <50 kg, and 2.5 mg/kg/day in children (maximum dose, 100 mg/day). Major concerns about the wide use of hexadecylphosphocholine include its teratogenic potential and its long half-life (approximately 150 h), which may facilitate the emergence of resistance. This agent is associated with high efficacy rates, even in cases unresponsive to antimonials (14, 49). Paromomycin (aminosidine) is an aminoglycoside with antileishmanial activity. In a phase III study of VL in India, this drug was associated with 94.6% cure rates, similar to that of amphotericin B (54). Adverse effects were more frequent in the paromomycin-treated group than in the amphotericin B-treated group (6% versus 2%, respectively); paromomycin-related adverse effects included elevated hepatic transaminases, ototoxicity, and pain at the injection site (54). Combinations of hexadecylphosphocholine with AmB, paromomycin, or pentavalent antimonials have been evaluated in an *in vivo* model, which revealed that the combinations of hexadecylphosphocholine with AmB or paromomycin were efficacious (50).

AmB is a polyene antifungal drug often used intravenously for systemic fungal infections. It was originally extracted from *Streptomyces nodosus*, a filamentous bacterium (33, 15). Currently, the drug is available as plain AmB, as a cholesteryl sulfate complex, as a lipid complex, and as a liposomal formulation (33). The latter formulations have been developed to improve tolerability for the patient but may show pharmacokinetic characteristics considerably different from those of plain AmB (33, 46).

The mechanism(s) of AmB resistance among fungi varies. The primary target of AmB is ergosterol in the cell membrane of fungi. The binding of AmB to sterols (ergosterol-containing membranes are more sensitive than cholesterol-containing membranes [9])

Received 10 January 2011 **Returned for modification** 23 March 2011
Accepted 30 October 2011
Published ahead of print 28 November 2011
Address correspondence to Pradeep Das, drpradeep.das@gmail.com.
B. Purkait and A. Kumar contributed equally to this article.
Supplemental material for this article may be found at http://aac.asm.org/.

doi:10.1128/AAC.00030-11

incorporated in artificial or cellular membranes results in disorganization of the membrane (5), possibly by formation of specific pores composed of small aggregates of AmB and sterol (56). These defects cause depolarization of the membrane and an increase in membrane permeability for protons and monovalent cations (8, 32). Recently, however, researchers found evidence that pore formation is not necessarily linked to cell death (2). The actual mechanism of action of AmB may be more complex and multifaceted. Another mechanism by which AmB could affect the cells is its auto-oxidation and subsequent formation of free radicals (32). AmB-induced cell injury might be associated with both ion movement and oxidative effects (8). If AmB-induced cell damage is linked to the generation of reactive forms of oxygen, the ability to decompose them should affect cell resistance to damage (7, 4). Kinetoplastids, comprising parasites of the genera *Crithidia*, *Trypanosoma*, and *Leishmania*, are devoid of catalase and glutathione peroxidase (6, 17, 19), and the removal of hydroperoxides in these parasites is presumed to rely mainly on the tryparedoxin pathway to regulate oxidative stress (39, 44). This pathway consists of a cascade of low-molecular-weight, thiol-specific oxidoreductases acting in an NADPH-dependent manner to detoxify peroxides in the following order: trypanothione reductase (TR) → trypanothione (TSH) → tryparedoxin → tryparedoxin peroxidase (11, 55). In antimonial resistance, it was shown that overexpression of tryparedoxin peroxidase is linked with resistance against oxidative stress (36). In trypanosomatids, a reduced form of trypanothione is involved in the maintenance of the intracellular reducing environment, substituting for the glutathione (GSH) found in most other organisms (18). The enzyme trypanothione reductase, absent from mammalian cells, is mainly responsible for keeping trypanothione reduced (17, 31). The rate-limiting enzymes for trypanothione biosynthesis are γ-glutamylcysteine synthetase (γ-GCS; encoded by the *gsh1* gene) and ornithine decarboxylase (ODC) (47). In *Leishmania tarentolae* isolates resistant to arsenite, buthionine sulfoximine (BSO), an inhibitor of γ-GCS, can partially revert the resistance phenotype (24, 47). Also, treatment of a glucantime-resistant *Leishmania tropica* line with BSO produced a thiol depletion that was accompanied by a substantial increase in the chemosensitivity to glucantime (1).

The ATP-binding cassette (ABC) transporters represent the biggest known superfamily of proteins, being present in all studied organisms, from archaebacteria to higher eukaryotes (26). In addition to their physiological function, translocating a high variety of substrates across the cellular membrane, ABC proteins have enormous medical relevance. Some of them are responsible for the multidrug resistance (MDR) phenotype during the treatment of cancer and infectious diseases, and others are involved in important genetic diseases. In *Leishmania* spp., three different classes of ABC transporters are known. It has been reported that two types of ABC transporters are involved in drug resistance mechanisms in *Leishmania* spp. (47): P-glycoprotein A (PgPA), which is homologous with the mammalian MDR-associated protein (MRP) cluster (involved in drug sequestration) (45), and MDR1, which is homologous with the mammalian PgP cluster (involved in drug efflux) (25). It has also been demonstrated that cotransfection of *gsh1* and PgPA in the revertant resulted in resistance levels that were higher than expected from the individual contribution of either gene (24).

Although AmB chemotherapy has been proven to be very successful in treatment of VL in India, due to the very high frequency of its use, emergence of drug-resistant cases is expected (53). We have encountered some AmB-unresponsive cases at the Rajendra Memorial Research Institute of Medical Sciences (RMRIMS), Bihar, India. Microbiological evolution of one such clinical isolate showed resistance in *in vitro* as well as *ex vivo* studies. Until now, no study of any AmB-resistant clinical isolate to understand the mechanism of resistance has been done. Therefore, the major objective of the present investigation is to understand the molecular mechanism of AmB resistance of the clinical isolate by investigating the involvement of membrane composition, drug efflux machinery, and the peroxide elimination cascade using clinical isolates of *Leishmania donovani*.

MATERIALS AND METHODS

Clinical isolates. Clinical isolates of VL were obtained from the splenic aspirates of AmB-responsive and -nonresponsive patients in the indoor ward facility of Rajendra Memorial Research Institute of Medical Sciences, Patna, Bihar, India. Briefly, the collected splenic aspirates were incubated in RPMI-1640 medium (Gibco) (pH 7.4) supplemented with 10% fetal bovine serum (FBS) (Gibco) and 1% of penicillin (50 U/ml)-streptomycin (50 mg/ml) solution (Sigma) at 25°C. The amastigotes from splenic aspirates were transformed into promastigotes, and they were maintained further in RPMI-1640 medium supplemented with FBS.

Cell line. The THP1 cell line was maintained in a 25-cm^2 flask (Corning) in Dulbecco's modified Eagle medium (DMEM) (Sigma) supplemented with 10% FBS and antibiotics (streptomycin and penicillin) in a humidified 5% CO_2/air atmosphere at 37°C.

Characterization and clonal selection of clinical isolates. Clinical isolates were confirmed as *Leishmania* spp. by amplification of kinetoplast DNA (kDNA) using a kDNA gene-specific primer (F, 5′-TCTGTGGCC CATTTGTTGTA-3′, and R, 5′-CATTTTTGGGTTTTCGGAGA-3′). The isolates were then clonally selected by growing them on NNN agar slant medium. The single colonies formed on the agar slant were further grown separately in RPMI-1640 medium.

***In vitro* drug sensitivity assay.** *In vitro* drug sensitivity was determined by incubating 2×10^6 parasites in RPMI-1640 medium (supplemented with 10% FBS) with different concentrations of AmB and at 1-day intervals for 6 consecutive days. Parasites were not treated with AmB in the control experimental set. Viable cells were counted in a hemocytometer (Rohem) by the trypan blue (Sigma) (0.5 mg ml^{-1}) exclusion method, and the 50% lethal doses (LD_{50}) were determined for both the AmB-resistant and AmB-sensitive strains. There were three replicates in each test, and the data are the means and the standard deviations (SDs) of three experiments.

MTT assay. The 3-(4,5-dimethyl-2-thiazolyl)-2,5-diphenyl-2H-tetrazolium bromide (MTT) assay is a quantitative colorimetric assay for measurement of metabolically active cells. This assay is based on cleavage of the yellow tetrazolium salt, MTT (Sigma), which forms water-insoluble, dark blue formazan crystals, and this cleavage happens in living cells only because of the mitochondrial enzyme succinate dehydrogenase. To determine the LD_{50} of AmB using an *in vitro* drug sensitivity assay, 10 μl of MTT solution (5 mg/ml) was added for each 100 μl of untreated or drug-treated parasite culture. After addition of MTT, the cultures were incubated at 22.4°C for 3 h and subsequently incubated with 200 μl of MTT solubilization buffer. Absorbance was recorded at 570 nm using a UV-visible spectrophotometer (Hitachi, Japan). The MTT assay was also performed to quantify the proportion of metabolically active cells after the addition of inhibitors (both the thiol metabolic pathway and ABC transporter inhibitors) and a reactive oxygen species (ROS) scavenger, 6-hydroxy-2,5,7,8-tetramethylchroman-2-carboxylic acid (Trolox) (20 mM) (Sigma), for untreated and AmB-treated parasites. There were three replicates in each test, and the data are the means and SDs of three experiments.

Cell cytotoxicity assay. THP1 cells were counted in an improved Neubauer chamber using the vital stain trypan blue, and 10^4 cells/well were placed in a 96-well plate with different concentrations of AmB. After 48 h of incubation, the medium was removed, 200 μl of fresh supplemented medium and 20 μl of alamarBlue (Sigma) were added, and the absorbance was measured at 550 nm. There were three replicates in each test, and the data are the means and SDs of three experiments.

***Ex vivo* assay.** An *ex vivo* assay was performed using a modification of the method described by Mendez et al. (40). Briefly, 10^4 THP1 cells/well were cultured in 8-well Lab-Tek chambers (Nunc, Roskilde, Denmark). Once macrophages were adhered, 10^5 stationary-phase *Leishmania* promastigotes were added to each well and maintained at 33°C in 5% CO_2 overnight. Noninternalized promastigotes were eliminated, and different concentrations of AmB were added to the wells and incubated for 48 h. Slides were then fixed and stained (Giemsa), and the number of amastigotes/100 cells was determined. LD_{50} values for both resistant and sensitive parasites were calculated. There were three replicates in each test, and the data are the means and SDs of three experiments.

K^{+i} level. The intracellular K^+ (K^{+i}) levels of AmB-treated (0.125 μg/ml) resistant and sensitive parasites were determined using 5 mM potassium-binding benzofuran isophthalate acetoxymethyl (PBFI-AM; Sigma) as a cell-permeant probe and an LS55 spectrofluorimeter (Perkin Elmer). Fluorescence in the parasites was analyzed by excitation at 370 nm, and emission was registered at 540 nm.

Membrane fluidity. Diphenylhexatriene (DPH) has been used as a fluorescence probe to measure the fluidity of membranes (34, 35). In brief, a stock solution of the probes (2 mM DPH in tetrahydrofuran) was stored at 4°C in the dark. For labeling, the 2 mM final concentration of DPH was added to both AmB-resistant and AmB-sensitive promastigotes (2×10^6 cells/ml) and incubated for 45 min at 37°C. The suspension was centrifuged, washed, resuspended in phosphate-buffered saline (PBS; pH 7.2), and fixed with 4% paraformaldehyde. The fluorescence anisotropy was immediately measured in an LS55 spectrofluorimeter (Perkin Elmer). The excitation and emission wavelengths were 360 nm and 430 nm, respectively. Fluorescence anisotropy was calculated by the following equation: $I_{vv} - (GF \times I_{vh})/I_{vh} + (2 \times GF \times I_{vh})$. Here, I_{vv} and I_{vh} are the intensities with polarizers that are vertical and vertical (excitation and emission, respectively) and vertical and horizontal, respectively. The grating factor (GF) is specific for the instrument and is defined by the ratio of I_{hv} to I_{hh}, where I_{hv} and I_{hh} are the intensities with polarizers that are horizontal and vertical (excitation and emission, respectively) and horizontal and horizontal, respectively. The polarization value of DPH fluorescence was used as a measure of membrane fluidity, since decreased anisotropy indicates an increase in membrane fluidity (29).

Extraction and analysis of free sterols. Promastigotes were grown as described above in three Erlenmeyer flasks in a total volume of 1 liter of culture medium. For cell treatment, a volume of the drug corresponding to an appropriate final concentration was added to 10% dimethyl sulfoxide in water, and cultures were incubated at 27°C for various times at 150 rpm in an orbital incubator (Gallenkamp). Cells were harvested, washed, and pooled, and the pellet was resuspended in 20 ml of dichloromethane-methanol (2:1, vol/vol) for about 24 h at 4°C. After centrifugation (11,000 × *g*, 1 h, 4°C), the extract was evaporated under vacuum. The residue and the pellet were saponified with 30% KOH in methanol at 80°C for 2 h. Sterols were extracted with *n*-hexane, which was thereafter evaporated, and the residue was dissolved in dichloromethane. An aliquot of clear yellow sterol solution was added to 2 volumes of *N*,*O*-bis(trimethylsilyl)trifluoroacetamide (BSTFA), and the sealed tubes were heated at 80°C for 1 h. The trimethylsilyl (TMS) ethers of the sterols were subjected to gas chromatography/mass spectrometry (GC/MS) analysis by following previously described methods with some modifications (21, 30). GC was performed with a Varian model 3400 chromatograph equipped with DB5 columns (methyl-phenylsiloxan ratio, 95/5; dimensions, 30 m by 0.25 mm). The gas carrier was He (1 ml/min). Analysis conditions were as follows: the column was kept at 270°C, the injector was kept at 300°C (splitless), and the detector was kept at 300°C (isothermic conditions for sterols). The linear gradient for methyl esters was from 150 to 180°C at 10°C/min. The MS conditions were 280°C, 70 eV, and 2.2 kV.

Determination of intracellular AmB content in treated promastigotes. AmB-resistant and -sensitive promastigotes were cultured in 25-cm^2 flasks at an initial concentration of 1×10^6 cells/ml in RPMI-1640 medium supplemented with 10% FBS. Flasks were kept at 22.5°C with and without AmB (0.125 μg/ml) for the desired time periods. Promastigotes were harvested by centrifugation and washed twice with large volumes of cold PBS (pH 7.2). Pellets were resuspended in an aqueous solution of 20 mM cholic acid for 24 h at 4°C and then centrifuged (11,000 × *g*, 1 h, 4°C). An equal volume of cold ethanol was added to the supernatant, and the mixture was kept in an ice bath for 1 h to precipitate the proteins. The samples were then centrifuged (11,000 × *g*, 1 h, 4°C), and the clear supernatants were analyzed by high-performance liquid chromatography (HPLC) (Hitachi) for AmB determination.

HPLC analysis. Reverse-phase chromatography analysis on a C_{18} reversed-phase column (4.6 by 250 mm) (Zorbax) was performed with an HPLC (Hitachi). The detection was at 408 nm, corresponding to the maximum absorbance for AmB. An isocratic mobile phase of acetonitrile-water-acetic acid (45:51:5) was delivered at a flow rate of 1 ml/min. Standard concentrations of 0.0125, 0.125, 0.25, 0.5, 1, and 5 μg/μl were made by dissolving AmB in the mobile phase or in methanol.

Drug efflux measurement. *Leishmania* promastigotes treated with the drug were harvested as described above and transferred to fresh, drug-free medium after different time points and incubated for 2 h prior to extraction. The AmB efflux was measured using HPLC (Hitachi) in a manner similar to that described above.

Semiquantitative RT-PCR and real-time PCR. Reverse transcription was performed using 0.2 mg total RNA from untreated *L. donovani* cells and 0.125 μg/ml AmB-treated *L. donovani* cells incubated for 8 h using an anchored oligo(dT) (H-dT11M, where M represents A, C, or G; GenHunter). The synthesized cDNAs were amplified by PCR for specific genes, *viz.*, MDR1, PgPA, ODC, spermidine synthase (SPS), γ-GCS, trypanothione synthetase (TryS), TR, cytoplasmic tryparedoxin (cTXN), cytoplasmic tryparedoxin peroxidase (CTP), mitochondrial tryparedoxin (mTXN), mitochondrial tryparedoxin peroxidase (MTP), and *S*-adenosyl-L-methionine:C-24-Δ-sterolmethyltransferase (SCMT) A and B. The forward (F) and reverse (R) primers of SCMT A and SCMT B were designed on the basis of the 3′ untranslated region (UTR) (48). In all PCRs after initial denaturation at 94°C for 5 min, targeted genes were amplified by 25 amplification cycles (94°C for 30 s, 56°C or 58°C for 30 s, and 72°C for 1 min), followed by a final extension at 72°C for 5 min. All PCRs were performed for 25 cycles, which was within the linear range of amplification of the corresponding mRNA species. The products were run on 1.5% agarose gel, stained with ethidium bromide, and finally documented and quantified using the Bio-Rad gel documentation system and associated Quantity One software. All the reverse transcription PCR (RT-PCR) products were normalized with respect to the alpha-tubulin (a-tub) RT-PCR product. These semiquantitative data were validated by quantitative real-time PCR, which was performed in the LightCycler 480 (Roche) using SYBR green (Roche) chemistry. The cycling conditions were as follows: 1 cycle at 95°C for 3 min and 40 cycles of 95°C for 15 s (denaturation), 58°C for 30 s (annealing), and 72°C for 30 s (extension). The fluorescence signal was captured at the end of each cycle using the SYBR channel (490-nm wavelength for excitation and 525-nm wavelength for emission). Results are the target/reference ratios of each sample, normalized by the target/reference ratio of the calibrator. Here, the target/reference value of sensitive parasites was used as the calibrator and the alpha-tubulin was used as the reference.

The primers used for both semiquantitative RT-PCR and quantitative real-time PCR were as follows: for MDR1, 5′-AATGCTCTTGAGCCTCA-3′ (F) and 5′-CTTCCAGTTGACTACATTCC-3′ (R); for PgPA, 5′-TCAATCAGTCAAATGTCTTGC-3′ (F) and 5′-GAATGTCAACTTTCCTACTCC-3′ (R); for ODC, 5′-GCACGCGCTTCTCATGAACGTATT-3′ (F)

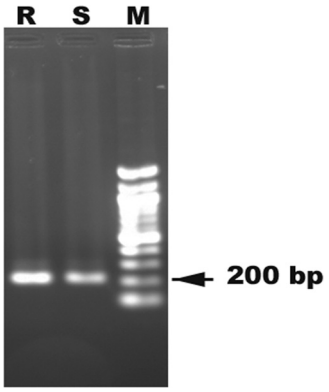

FIG 1 kDNA amplification of both resistant and sensitive parasites. Lane M, S, and R represent a 100-bp marker, amplified kDNA from a sensitive parasite, and amplified kDNA from a resistant parasite, respectively.

and 5′-CGAAGAGGATGCAGTTGAAGCTGT-3′ (R); for SPS, 5′-ACTTCTACACGAATGTGCTCCGCA-3′ (F) and 5′-CATTGCGTACTTGACCGTGGCAAA-3′ (R); for γ-GCS, 5′-AGCGATAAACCGCTCGTACTGTGA-3′ (F) and 5′-ATGTTGTCAAAGTGCTCCGTGTGC-3′ (R); for TryS, 5′-TGTCATGAGCGAATGACCAACCGAT-3′ (F) and 5′-GCTTGCCATTCAACAAACGTCAGGT-3′ (R); for TR, 5′-AATGAGGACGGCTCGAATCACGTT-3′ (F) and 5′-ATGGCGTAGATGTTGTCCACCGAT-3′ (R); for cTXN, 5′-AAGCTAAACACGCAGGTTGTTGCG-3′ (F) and 5′-ATACCGGATTCCTCGATCAGCACA-3′ (R); for CTP, 5′-CCAACGGCAGCTTCAAGAAGATCA-3′ (F) and 5′-TGAAGTCGAGCGGGTAGAAGAAGA-3′ (R); for mTXN, 5′-GCTTCACTCCGAAGCTCGTTGAAT-3′ (F) and 5′-AGTACTCCATGAAAGCGTCGGCCT-3′ (R); for MTP, 5′-AAGCTAAACACGCAGGTTGTTGCG-3′ (F) and 5′-TCGATCAGCACACCATAGTCACGA-3′ (R); for SCMT A, 5′-CATCTTCCCTCCCTTTCCTC-3′ (F) and 5′-CCGCATGAACAACAGAGAGA-3′ (R); and for SCMT B, 5′-TGTCCAGTAGTCCCGGAAAC-3′ (F) and 5′-CGGCGATGATAGTGATGTTG-3′ (R).

Determination of total intracellular reduced thiol content. The level of total intracellular thiol was measured in deproteinized cell extracts for both resistant and sensitive strains. The late-log-phase cells were harvested, washed with a buffer (0.14 M Na_3PO_4, 0.14 M K_3PO_4, 0.14 M NaCl, and 3 mM KCl) (pH 7.4), and suspended in 0.6 ml of 25% trichloroacetic acid. After 10 min on ice, the denatured protein and cell debris were removed by centrifugation in a microcentrifuge for 10 min at 4°C. The thiol content of the supernatant solution was determined with 0.6 mM 5,5′-dithio-bis(2-nitrobenzoic acid) (DTNB, Ellman's reagent) (16) in 0.2 M Na_3PO_4 buffer (pH 8.0). The concentration of DTNB derivatives of thiols was estimated spectrophotometrically at 412 nm. There were three replicates in each test, and the data are the means and SDs of three observations.

Detection of accumulation of reactive oxygen species. Intracellular oxidant levels were determined by the use of 2′,7′-dichlorodihydrofluorescein diacetate (H_2DCFDA) (Sigma), which is oxidized inside the cell to the fluorescent dichlorofluorescein (DCF). AmB-treated (0.125 μg/ml) sensitive and resistant parasites (2×10^6 of each set) were incubated after the desired time intervals with 0.4 mM (final concentration) H_2DCFDA for 15 min in the dark. The cells were washed once in PBS (pH 7.2) and were harvested and lysed in lysis buffer (1% SDS and 1% Triton X-100 in 10 mM Tris), and the fluorescence intensity was measured in the supernatant using an LS55 spectrofluorimeter (Perkin Elmer), with excitation measured at 504 nm and emission at 529 nm. The measured fluorescence intensity was directly proportional to the accumulation of ROS. The reagent blank was prepared with 0.4 mM (final concentration) H_2DCFDA in lysis buffer. The accumulation of ROS has also been measured in the presence of the ROS scavenger 6-hydroxy-2,5,7,8-tetramethylchroman-2-carboxylic acid (Sigma). There were three replicates in each test, and the data are the means and SDs of three observations.

Inhibitor assay. Verapamil, an ABC transporter inhibitor, BSO, an inhibitor of γ-GCS, and difluoromethylornithine (DFMO), an inhibitor of ODC, were added at concentrations of 5 μM each to study the effect of ABC transporters and thiol metabolic pathway inhibitors in strain reversal. They were added to the resistant parasites and incubated for 2 h at 23°C in a biological oxygen demand (BOD) incubator prior to AmB treatment. The parasites were subsequently washed with PBS (pH 7.2) and treated with AmB. Three experimental sets were prepared for the inhibitor assay: parasites preincubated with only verapamil, parasites pretreated with BSO and DFMO, and parasites pretreated with verapamil, BSO, and DFMO simultaneously. The LD_{50} of AmB, intracellular thiol content, intracellular AmB content, and efflux of AmB in a drug-free medium were recorded. There were three replicates in each test, and the data are the means and SDs of these three observations.

RESULTS

Characterization of clinical isolates. The parasites isolated from the splenic aspirates of VL patients were confirmed as *Leishmania* species by kDNA amplification (Fig. 1), and they were also demonstrated to be axenic, as they are clonally selected in NNN blood agar medium.

Confirmation of AmB-resistant and -sensitive nature of clinical isolates. The LD_{50} value for the resistant strain was found to be 8-fold higher than that of the sensitive strain, as demonstrated by both *in vitro* and *ex vivo* drug sensitivity assays (Table 1). We have also studied the cross-resistance property of AmB-resistant clinical isolates to structurally and functionally unrelated drugs and showed no significant cross-resistance toward other drugs, such as hexadecylphosphocholine, sodium antimony gluconate (SAG), paromomycin, and sodium stibogluconate (data not shown).

Increased membrane fluidity for the resistant strain. The change in plasma membrane sterol content and composition must alter the physical state of the plasma membrane. DPH, a hydrophobic probe, shows a double hard-cone wobbling movement to incorporate a hydrocarbon inside the membrane bilayer, and orientation of the probe in the membrane is related to the physical state of the lipid bilayer (10). The emission anisotropy value of DPH fluorescence was used as a measure of membrane fluidity. Figure 2A demonstrated that the emission anisotropy value of AmB-resistant *Leishmania* promastigotes was ~2.5 times lower than that of the sensitive promastigotes, indicating differences in the trimethylammonium (TMA)-DPH environment within the plasma membranes of these cells. The membrane of AmB-resistant cells is therefore more fluid than that of AmB-sensitive cells. This change in membrane fluidity is probably a consequence of the resistance-induced modification of membranous lipid metabolism.

Decreased $K^{+}{}_{i}$ level for the sensitive strain. The AmB-treated sensitive promastigotes demonstrated an ~2-fold decrease in the

TABLE 1 Comparison of LD_{50} of AmB-resistant and -sensitive clinical isolates in the presence of AmB

Drug sensitivity assay	LD_{50}[a] (μg/ml) of indicated parasites	
	AmB-sensitive	AmB-resistant
In vitro	0.125	0.837
Ex vivo	0.2	1.57

[a] LD_{50}, 50% lethal dose.

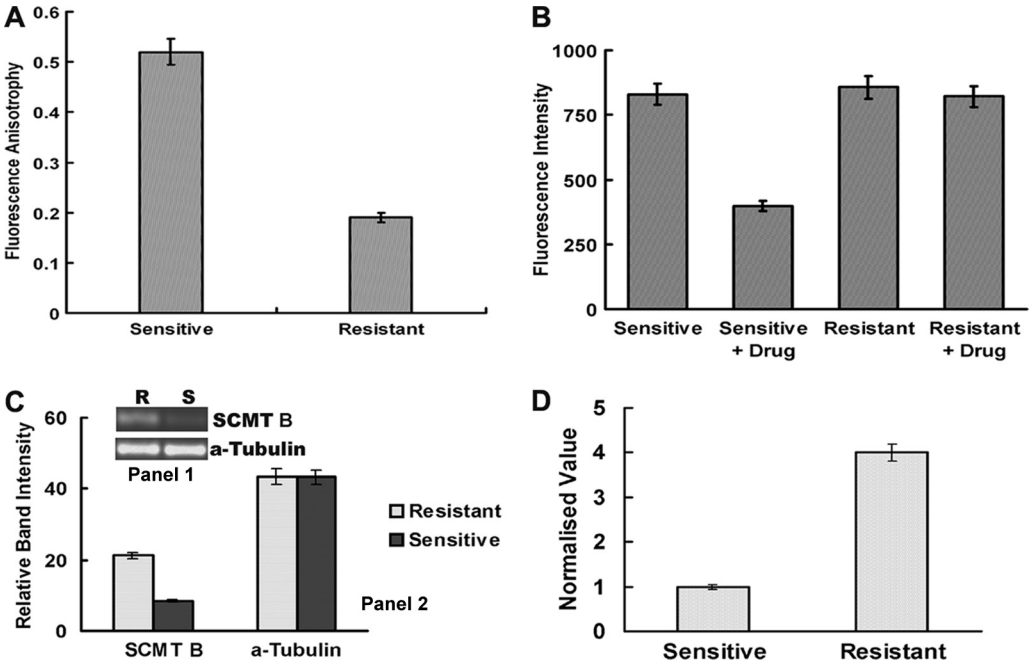

FIG 2 (A) Determination of membrane fluidity of resistant and sensitive parasites. Membrane fluidity was measured by calculating fluorescence anisotropy of both parasites using DPH. There were three replicates in each test, and the data are the means and SDs of three independent experiments. (B) Intracellular K^+ (K^{+i}) levels of AmB-treated and untreated resistant and sensitive parasites. K^{+i} levels were analyzed spectrofluorimetrically using PBFI-AM. There were three replicates in each test, and the data are the means and SDs of three independent experiments. (C) Semiquantitative RT-PCR analysis of expression levels of SCMT B in resistant and sensitive parasites. Ethidium bromide-stained PCR products were photographed, and the images were analyzed densitometrically. An alpha-tubulin PCR was conducted to show uniform expression of a housekeeping gene in both parasites. Data are the means and SDs of three independent experiments. Panel 1 shows the gel images; panel 2 is a graphical representation of the densitometric data. (D) Quantitative real-time PCR analysis of expression levels of SCMT B for resistant and sensitive *L. donovani* strains. Data are the target/reference ratios of each sample, normalized by the target/reference ratio of the calibrator. Here, the target/reference value of the sensitive parasite was used as the calibrator and alpha-tubulin was used as the reference.

K^{+i} level compared to that of resistant promastigotes (Fig. 2B). The lower the K^{+i} level is, the higher the K^+ leakage will be and, consequently, the higher the membrane depolarization will be. Therefore, the membrane of the sensitive strain was more depolarized than that of the resistant strain after AmB treatment.

Expression pattern of SCMT gene. SCMT (*S*-adenosyl-L-methionine:C-24-Δ-sterol methyltransferase) is an important enzyme in the sterol biosynthetic pathway, as it performs C-24 transmethylation, which is a key step in production of ergosterol. SCMT has two transcripts, SCMT A and SCMT B (48). We have found that SCMT A is absent in AmB-resistant parasites and expressed in sensitive parasites (data not shown), but the SCMT B was more highly expressed (~2.5-fold higher) in the AmB-resistant parasites than in the AmB-sensitive parasites (Fig. 2C). These data have again been confirmed by quantitative real-time PCR (Fig. 2D). This result indicates an altered sterol biosynthesis in the resistant strain, which has a lower affinity for AmB.

Sterol analysis of sensitive and resistant parasites by GC/MS. Sterol composition and content reported to be involved in the laboratory-derived AmB resistance of *L. donovani* parasites (38) were analyzed through GC/MS to understand sterol's involvement in conferring AmB resistance in clinical isolates of *L. donovani*. Recorded mass spectra (see the supplemental material) were used to identify the sterols (21, 22, 30, 37, 38). The fragment ions at *m/z* 458 (M^+), *m/z* 468 (M^+), *m/z* 454 (M^+), and *m/z* 468 (M^+) are indicative of cholesterol, ergosterol, cholesta-5,7,24-trien-3β-ol, and ergosta-5,7,24(28)-trien-3β-ol, respectively (see the supplemental material). GC/MS analysis showed that ergosterol (28%) and its isomer ergosta-5,7,24(28)-trien-3-β-ol (34%) are present in AmB-sensitive parasites, and these two components represent 62% of the total sterols in these parasites. In the case of AmB-resistant parasites, ergosterol is absent and the major sterol is cholesta-5,7,24-trien-3-β-ol (62%) (Table 2). Cholesterol is present in both parasites, as cholesterol is taken up from the culture medium, but it is not metabolized by the parasite in either AmB-resistant or -sensitive parasites. Mass spectra for the TMS ether derivatives are given in the supplemental material.

Expression levels of ABC transporters. The relative expres-

TABLE 2 Composition of free sterols in AmB-sensitive and -resistant *L. donovani* promastigotes

Sterol	Trr (min)[a]	% of total sterols in indicated parasites[b]	
		AmB-sensitive	AmB-resistant
Cholesterol	1	11	24
Ergosterol	1.29	28	–
Cholesta-5,7,24-trien-3β-ol	1.12	–	62
Ergosta-5,7,24 (28)-trien-3β-ol	1.48	34	–
Ergosta-7,24(28)-dien-3β-ol	1.53	–	–
Other sterols (not identified)		16	15

[a] Trr, time of retention relative to cholesterol in gas-liquid chromatography (GLC).
[b] –, not detected.

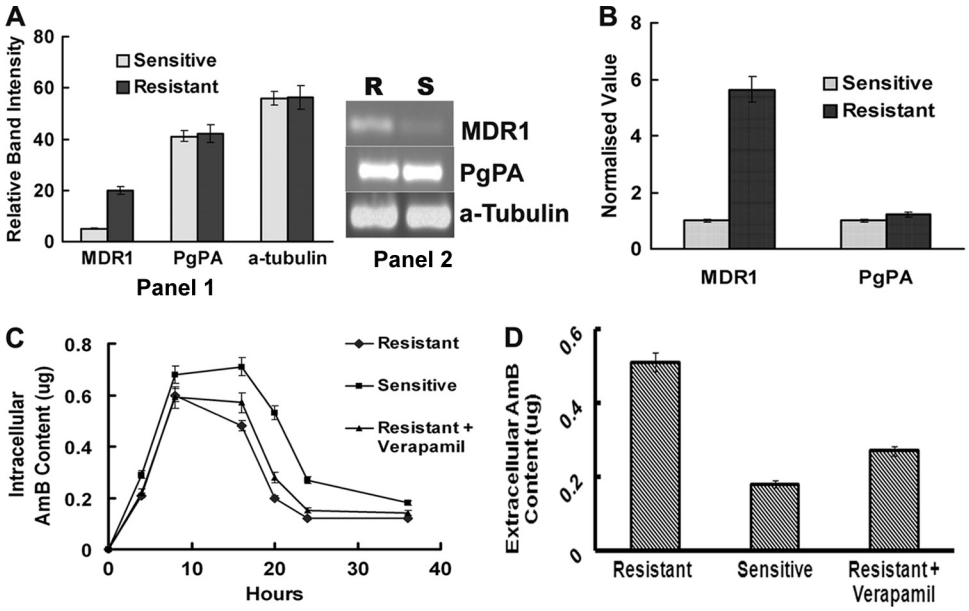

FIG 3 (A) Semiquantitative RT-PCR analysis of ABC transporters (MDR1 and PgPA) in AmB-treated resistant and sensitive *L. donovani* strains. Ethidium bromide-stained PCR products were photographed, and the images were analyzed densitometrically. An alpha-tubulin PCR was conducted to show uniform expression of a housekeeping gene in both parasites. Data are the means and SDs of three independent experiments. Panel 1 is a graphical representation of the densitometric data; panel 2 shows the gel images. (B) Quantitative real-time PCR analysis of expression levels of MDR1 and PgPA for AmB-treated resistant and sensitive *L. donovani* strains. Data are the target/reference ratios of each sample, normalized by the target/reference ratio of the calibrator. Here, the target/reference value of the sensitive parasite was used as the calibrator and alpha-tubulin was used as the reference. (C) Time kinetics of intracellular AmB accumulation in resistant and sensitive *L. donovani* strains. The intracellular AmB levels at different time points in the verapamil (MDR1 inhibitor)-treated resistant *L. donovani* strain have also been demonstrated. Intracellular AmB content was measured using reverse-phase HPLC. Values are the means and SDs of three independent experiments. (D) Efflux of AmB from AmB-treated sensitive and resistant *L. donovani* strains as well as from AmB-treated resistant *L. donovani* strains pretreated with verapamil. Extracellular AmB content was measured using reverse-phase HPLC. Values are the means and SDs of three independent experiments.

sion levels of the ABC transporters reported to be involved in drug efflux/sequestration in *Leishmania* have been explored to understand the involvement of ABC transporters in conferring AmB resistance. The expression levels of MDR1 (homologous with the mammalian PgP cluster) (25) and PgPA (homologous with the mammalian MRP cluster) (45) were investigated by semiquantitative reverse transcriptase PCR (Fig. 3A) and further confirmed by real-time PCR (Fig. 3B). The mRNA level of MDR1 was approximately 4-fold higher in the resistant strain than in the sensitive strain, whereas the mRNA level of PgPA was about the same in both strains.

Intracellular AmB content. The intracellular AmB content for drug-treated sensitive promastigotes was enhanced with an increase in incubation time, whereas that of the resistant strain increased slowly up to 8 h and decreased afterwards (Fig. 3C). It has also been observed that after 16 h of incubation, the intracellular AmB content of the sensitive promastigotes also starts to decrease significantly (Fig. 3C). We have also investigated the intracellular AmB content in the presence of verapamil, and the amount of intracellular AmB is lower than in uninhibited resistant parasites (Fig. 3C).

AmB efflux. AmB efflux from the sensitive and resistant parasites has been studied by incubating the cells in a drug-free medium after treatment with the drug for specific time frames. It was observed that after 8 h of incubation with AmB, the resistant strain demonstrates an ~2.9-fold-higher drug efflux than the sensitive strain (Fig. 3D).The AmB efflux for the resistant strain was also investigated in the presence of ABC transporter inhibitor verapamil. We found that the amount of AmB effluxed out in the drug-free medium is ~2-fold less after 8 h for the resistant strain when preincubated with verapamil (Fig. 3D).

Expression levels of thiol metabolic pathway genes. The expression levels of the important thiol metabolic pathway genes were investigated with late-log-phase cultures of AmB-treated resistant and sensitive parasites. The mRNA levels of the enzymes involved in biosynthesis of trypanothione and regulation of the reduced trypanothione level were found to be upregulated in the resistant strain compared to those in the sensitive strain. The expression levels of ODC, SPS, γ-GCS, TryS, and TR were found to be upregulated ~2.3-fold, ~2.2-fold, ~2.8-fold, ~2.2-fold, and ~2.5-fold, respectively, in the resistant strain compared to the levels in the sensitive strain (Fig. 4). The gene of the tryparedoxin cascade (both cytosolic and mitochondrial) involved in peroxide elimination was also demonstrated to be upregulated in the resistant strain compared to its level in the sensitive strain. The mRNA levels of cTXN, CTP, mTXN, and MTP were found to be upregulated ~2.7-fold, ~2.3-fold, ~3-fold, and ~2.7-fold, respectively, in the resistant strain compared to the levels in the sensitive strain (Fig. 4). The above data were again validated by real-time PCR, and we observed similar variations in the expression levels of the investigated genes (Fig. 5A).

Intracellular reduced thiol levels. The total intracellular reduced thiol content was measured using DTNB [5,5′-dithiobis(2-nitrobenzoic acid)] and was found to be ~2-fold higher in the resistant strain than in the sensitive strain (Fig. 5B). Total intracellular reduced thiol contents for both the resistant and sen-

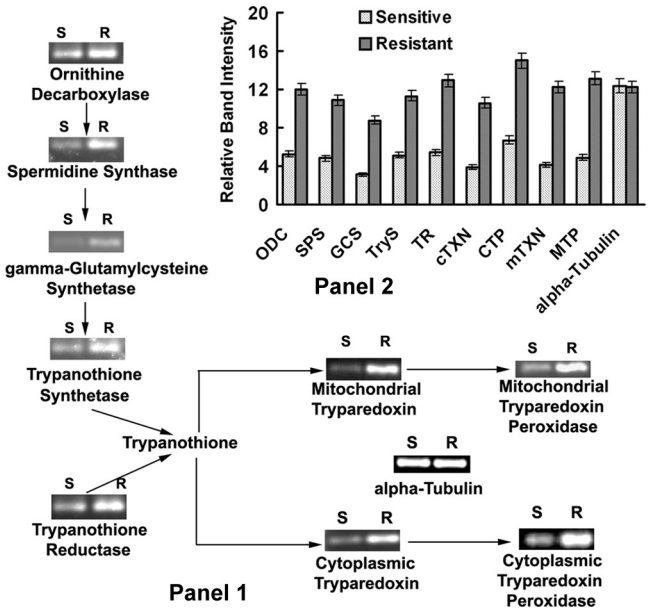

FIG 4 Determination of expression levels of thiol metabolic pathway enzymes in AmB-resistant and -sensitive *L. donovani* strains using semiquantitative RT-PCR. cDNAs prepared from resistant and sensitive parasites were subjected to semiquantitative RT-PCR using ornithine decarboxylase (ODC), spermidine synthase (SPS), γ-glutamylcysteine synthetase (γ-GCS), trypanothione synthetase (TryS), trypanothione reductase (TR), mitochondrial tryparedoxin (mTXN), mitochondrial tryparedoxin peroxidase (MTP), cytoplasmic tryparedoxin (cTXN), and cytoplasmic tryparedoxin peroxidase (CTP). Ethidium bromide-stained PCR products were photographed, and the images were analyzed densitometrically. An alpha-tubulin PCR was conducted to show uniform expression of a housekeeping gene in both parasites. Data are the means and SDs of three independent experiments. Panel 1 shows the gel images; panel 2 is a graphical representation of the densitometric data.

sitive strains had also been investigated in the presence of thiol metabolic pathway inhibitors BSO and DFMO. We found that the total reduced thiol content is decreased by ~1.4-fold in the resistant strain when preincubated with both inhibitors (Fig. 5B). However, in the case of coinhibition with both thiol metabolic pathway and ABC transporter inhibitors, effects similar to those described above (data not shown) were found.

Accumulation of ROS. The intracellular ROS production after AmB treatment was measured in a time-dependent manner using the nonfluorescent dye H_2DCFDA, which passively diffuses into cells, producing a polar diol by cleaving acetates of the dye using intracellular esterase, and gets retained inside the cells. The diol can then be oxidized by ROS to a fluorescent form, which can be measured for excitation at 480 nm and emission at 530 nm. The ROS levels in the resistant and sensitive strains were similar up to 16 h of incubation with the drug and were in the basal level (Fig. 5C). However, the ROS level for the sensitive strain started increasing steadily after 16 h and shot up to its maximum at 24 h and no significant change was observed in the resistant strain for the same time period (Fig. 5C). The ROS level of the sensitive strain was found to be ~4-fold higher than that of the resistant strain at 24 h of incubation with the drug (Fig. 5C). Treatment with the ROS scavenger (6-hydroxy-2,5,7,8-tetramethylchroman-2-carboxylic acid) significantly decreased the level of ROS in the sensitive strain (data not shown), and this, in turn, increased the rate of survival of the sensitive parasite, as the LD_{50} increased ~1.7-fold (Table 3). However, the ROS scavenger had no significant toxic effect on untreated resistant and sensitive parasites (data not shown).

Reversion of AmB resistance property by ABC transporter and thiol metabolic pathway inhibitors. Verapamil, an inhibitor

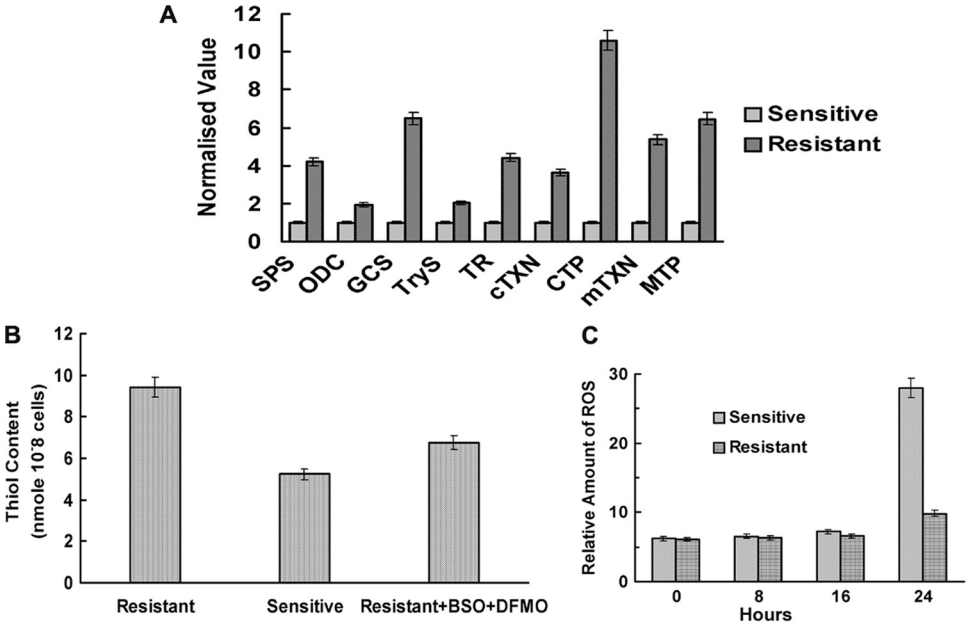

FIG 5 (A) Quantitative real-time PCR analysis of expression levels of thiol metabolic pathway enzymes (SPS, ODC, γ-GCS, TryS, TR, cTXN, CTP, mTXN, and MTP) for AmB-treated resistant and sensitive *L. donovani* strains using the same set of primers as described for the semiquantitative RT-PCR. Data are the target/reference ratios of each sample, normalized by the target/reference ratio of the calibrator. Here, the target/reference value of the sensitive parasite was used as the calibrator and alpha-tubulin was used as the reference. (B) Analysis of reduced intracellular thiol levels of AmB-treated sensitive and resistant *L. donovani* strains and resistant *L. donovani* strains treated with BSO, DFMO, and AmB. Thiol levels were measured spectrophotometrically using DTNB. Values are the means and SDs of three independent experiments. (C) Generation of intracellular ROS between 0 and 24 h in 8-h intervals for AmB-treated resistant and sensitive *L. donovani* strains. ROS generation was analyzed spectrofluorimetrically using H_2DCFDA. Values are the means and SDs of three independent experiments.

TABLE 3 Analysis of partial reversion of the resistant strain using ABC transporter and thiol metabolic pathway inhibitors and the ROS scavenger (6-hydroxy-2,5,7,8-tetramethylchroman-2-carboxylic acid)

Experimental set [strain + AmB + scavenger or inhibitor(s)]	LD_{50} (μg/ml)[a]	Fold change from LD_{50} of strain treated with only AmB[b]
Resistant strain + AmB	0.837	
Sensitive strain + AmB	0.125	
Sensitive strain + AmB + ROS scavenger	0.22	~1.7
Resistant strain + AmB + verapamil	0.43	~1.9
Resistant strain + AmB + BSO + DFMO	0.46	~1.8
Resistant strain + AmB + BSO + DFMO + verapamil	0.35	~2.4
Sensitive strain + AmB + verapamil	0.122	~1.01
Sensitive strain + AmB + BSO + DFMO	0.124	~1.0
Sensitive strain + AmB + BSO + DFMO + verapamil	0.120	~1.04

[a] LD_{50} of AmB in presence and absence of different inhibitors has been calculated from an *in vitro* drug sensitivity assay as described in Materials and Methods.
[b] Fold increase (in the presence of ROS scavenger) or decrease (in the presence of different inhibitors) from the LD_{50} value of the sensitive and resistant strains treated with only AmB.

of MDR1, had no significant toxic effect on the untreated sensitive and resistant parasites (data not shown). Preincubation with verapamil demonstrated partial reversion of the resistant property, as the LD_{50} of AmB for the resistant strain decreased ~1.9-fold (Table 3). However, the LD_{50} of the sensitive strain was not altered by preincubation with verapamil (the LD_{50} decreased ~1.01-fold). BSO and DFMO are inhibitors of γ-GCS and ODC, respectively, which are important rate-limiting enzymes of the thiol metabolic pathway. It has been demonstrated that BSO and DFMO have no significant toxic effect on the untreated sensitive and resistant parasites (data not shown). Preincubation with BSO and DFMO demonstrated a partial reversion of the resistant property, as the LD_{50} of AmB for the resistant strain decreased ~1.8-fold (Table 3). However, the LD_{50} of the sensitive strain did not change significantly by preincubation with the same inhibitors (the LD_{50} decreased ~1-fold). Coinhibition with both thiol metabolic pathway and ABC transporter inhibitors demonstrated a much larger decrease in the LD_{50} value (~2.4-fold) for the resistant strain than did inhibition with either ABC transport inhibitors or thiol metabolic pathway inhibitors (Table 3), whereas the decrease in the LD_{50} value was insignificant for the sensitive strain (~1.04-fold) (Table 3). Therefore, coinhibition has a much more potent effect on the partial strain reversion.

DISCUSSION

In this study, an attempt was made for the first time to understand the mechanism of resistance developed by clinical isolates of *Leishmania donovani* against AmB. The clinical isolates obtained from the VL patients were axenic, as they were selected in NNN blood agar medium and characterized by kDNA amplification (Fig. 1). The resistant or sensitive nature of the clinical isolates was confirmed by both *in vitro* and *ex vivo* drug sensitivity assays (Table 1). The resistant isolates were stable even after being exposed to the drug. In addition, the resistant line did not show cross-resistance to paromomycin, hexadecylphosphocholine, or sodium stibogluconate, but a low level of resistance to sodium antimony gluconate (SAG) was observed (data not shown). These results suggest that the resistance to AmB may be related to the chemical structure of the drug.

Sterols of *Leishmania* species have been previously studied, and common characteristics in biosynthetic pathways have been found between *Leishmania* species and fungi (22, 23). It has earlier been reported that in a laboratory-derived AmB-resistant *Leishmania* promastigote, ergosterol is replaced by a precursor, cholesta-5,7,24-trien-3β-ol (38). This probably results from a defect in C-24 transmethylation due to a loss of function of SCMT (12). According to Pourshafie et al. (48), SCMT has two transcripts, SCMT A and SCMT B. SCMT A is absent and SCMT B is highly expressed in AmB-resistant *L. donovani*. However, SCMT B has no spliced leader sequence and translation may be prevented, which could be the cause of the absence of sterol transmethylation (48). Our findings also demonstrated that SCMT A is absent and SCMT B is overexpressed in the AmB-resistant parasites compared to levels in sensitive parasites (Fig. 2C and D) and hence indicate the presence of an altered sterol (with a defect in C-24 transmethylation) in the resistant strain (12). To confirm our hypothesis, we analyzed the sterol compositions of both the AmB-resistant and -sensitive parasites through a standard GC/MS technique, and the mass spectra for TMS ether derivatives (see the supplemental material) were used to identify the structure of the sterols. Four different sterols have been identified on the basis of the fragment ions of the mass spectra (for the pattern of fragmentation, see references 21, 22, 30, 37, and 38). We found that ergosterol was the major sterol present in the sensitive strain, while in AmB-resistant promastigotes, the major sterol was cholesta-5,7,24-trien-3β-ol (Table 2) and no ergosterol was detected (Table 2). AmB-resistant *Leishmania* species are therefore defective in C-24 transmethylation of C-27 sterols. It has been reported (using lecithin liposome as a biometric model) that interaction between AmB and the membrane needs the ordered state (low fluidity) of the membrane (27). Membrane fluidity is dependent on the sterol and phospholipid composition (3, 13). According to Mbongo et al. (38), fatty acid composition is not significantly affected by resistance, and the predominant effect on membrane fluidity could be ascribed to cholesta-5,7,24-trien-3β-ol. It has been reported that fluorescence anisotropy is inversely proportional with the membrane fluidity (29). Fluorimetric analysis demonstrated lower anisotropy in the motion of the diphenylhexatriene fluorescent probe, which indicated a higher fluidity of the membrane for the resistant strain than for the sensitive strain (Fig. 2A). It was also demonstrated earlier that cholesterol decreased the order of dipalmitoyl-lecithin liposomes by reducing interactions between hydrocarbon chains of phospholipids (27). In AmB-resistant promastigote membranes, cholesta-5,7,24-trien-3β-ol could act similarly and make the membrane less ordered. These observations suggest that the high membrane fluidity and less-ordered state of the membranes of AmB-resistant parasites are mainly due to the presence of cholesta-5,7,24-trien-3β-ol instead of ergosterol. Therefore, altered sterol composition and increased membrane fluidity of the resistant strain probably make its membrane less ordered and, in turn, decrease binding affinity of AmB to the membrane.

Sokol-Anderson et al. (52) had reported earlier that sensitivity to AmB was measured as a loss of $K^{+}{}_{i}$ after exposure to AmB in fungi. We have also found that after AmB treatment, $K^{+}{}_{i}$ content is lower in the sensitive strain than in the resistant strain (Fig. 2B).

This lower membrane permeability of the monovalent cations for the resistant parasites may lead toward less membrane depolarization.

The reduced binding of AmB to the membrane of the AmB-resistant parasites can also lead toward lower AmB uptake (38). We have found that the intracellular AmB content is lower in the resistant strain than in the sensitive strain after 8 h of incubation with the drug (Fig. 3C). We have also observed a higher AmB efflux rate for the resistant strain than the sensitive strain (Fig. 3D). Therefore, lower intracellular AmB content in the resistant parasite than in the sensitive parasite may be a result of both impaired AmB uptake due to the absence of ergosterol in the AmB-resistant parasite (Table 2) and upregulated drug efflux machinery of the resistant parasite. To validate the involvement of drug efflux machinery, we investigated the expression levels of the ABC transporters (PgPA, involved in sequestration of the drug inside the vesicles [45], and MDR1, involved in efflux of the drug [25]) which are reported to be involved in drug resistance in leishmaniasis (47) in both the resistant and sensitive strains and which may be involved in AmB efflux. In our study, we have observed that the mRNA level of MDR1 is ~3-fold higher in resistant promastigotes than in sensitive promastigotes, although the mRNA levels of PgPA in each strain are similar (Fig. 3A and B). Therefore, the AmB efflux may correlate with the higher MDR1 expression level in the resistant strain.

Lamy-Freund et al. reported that AmB could affect cells by generating free radicals after auto-oxidizing itself (32). In the present study, we investigated the intracellular ROS levels for both resistant and sensitive promastigotes after AmB treatment to predict whether ROS is the key molecule for AmB-mediated cell death. The ROS level of the sensitive strain was found to be ~3-fold higher than that of the resistant strain at 24 h of incubation with the drug (Fig. 5C). Lower intracellular AmB content for the resistant parasite than for the sensitive parasite probably contributes toward this lower ROS level. Moreover, the resistant parasite may have overexpressed ROS scavenging machinery. Earlier studies have demonstrated that if AmB-induced cell damage is related to generation of ROS (41), the cell's resistance to damage might depend on its ability to decompose them efficiently (4, 7). It had earlier been reported that kinetoplastids detoxify hydroperoxides mainly by the tryparedoxin pathway (39, 43). To investigate the involvement of the tryparedoxin cascade in ROS scavenging, the expression levels of different thiol metabolic pathway genes were investigated in both resistant and sensitive parasites. We observed an upregulation in the mRNA levels of the enzymes involved in trypanothione biosynthesis and of the enzymes regulating the reduced trypanothione level in the resistant strain compared to those of the sensitive strain (Fig. 4 and 5A). This result correlates with the report by Lin et al. that overexpression of tryparedoxin peroxidase is linked with resistance against oxidative stress (36). Low-molecular-mass thiol also plays an important role in the defense against oxidative damage caused by oxidants (42, 47). Thus, in the present study, total intracellular thiol content (reduced) has also been investigated and we have found ~2-fold-higher thiol levels in the resistant strain than in the sensitive strain (Fig. 5B). Therefore, it is predicted that the ROS generated by the auto-oxidation of AmB may be decomposed by the end product of a highly active thiol metabolic pathway, i.e., tryparedoxin peroxidase in the resistant strain, and may help in conferring resistance. In addition to the tryparedoxin cascade, increased thiol levels in the resistant parasite may also be involved in better antioxidant defense. However, the sensitive strain, devoid of upregulated detoxifying machinery, is unable to combat the oxidative stress and undergoes ROS-dependent killing. This ROS-dependent cell death can again be confirmed by pretreatment of the sensitive strain with an ROS scavenger, causing the strain to demonstrate an increased LD_{50} for the drug (Table 3).

We have also demonstrated the effect of ABC transporter and thiol metabolic pathway inhibitors on the resistant strain to find out whether they have any effect on partial reversion of its resistant phenotype to a sensitive phenotype. Verapamil had been reported earlier to inhibit the efflux of drugs through ABC transporters (20). Similar inhibitory effects of verapamil had also been found in *Trypanosoma* and laboratory-derived resistant *L. donovani* isolates (43). In our study, we have found that verapamil (an inhibitor of MDR1) partially reverses the AmB resistance phenotype, a result which has been demonstrated by partial inhibition of AmB efflux (Fig. 3C and D) and a decreased LD_{50} value (~1.9-fold) (Table 3) for the resistant parasites. In trypanosomatids, trypanothione is the key molecule involved in maintaining the optimal intracellular reducing environment (18). The enzymes γ-GCS and ODC catalyze the rate-limiting step of trypanothione biosynthesis (47). In our present study, we have used BSO and DFMO for inhibiting the effects of γ-GCS and ODC, respectively, and found that the resistant phenotype partially reverts back to a sensitive phenotype, a result which has been demonstrated by decreased intracellular thiol content (~1.4-fold) (Fig. 5B) and LD_{50} values (~1.8-fold) (Table 3) for the resistant strain pretreated with thiol metabolic pathway inhibitors. This result correlates with the report that BSO can partially revert the resistant phenotype (1, 24). In our study, we have also examined the effect of coinhibition with both thiol metabolic pathway inhibitors and ABC transporter inhibitors on the resistant strain. We have found that coinhibition has a more potent effect than inhibition with either ABC transporter inhibitors or thiol metabolic pathway inhibitors in reversing the resistant property of the resistant strain, as demonstrated by an ~2.4-fold decrease in the LD_{50} value during coinhibition (Table 3), compared to ~1.8-fold and ~1.9-fold decreases for thiol metabolic pathway and ABC transporter inhibitors, respectively (Table 3). This may indicate a synergistic involvement of both drug efflux and ROS scavenging machinery in conferring AmB resistance.

Taken together, it is concluded that the absence of ergosterol in the resistant parasite's membranes and the upregulated AmB efflux and ROS scavenging machinery are having a cumulative effect in conferring resistance against AmB to the *Leishmania* parasite. The affinity of AmB for the membrane in the resistant parasite is less, owing to its altered membrane composition, and concomitantly, it reduces the amount of AmB taken up. Moreover, the overexpressed drug efflux machinery is allowing a higher efflux rate for AmB from the resistant parasite. As a result, the intracellular AmB content of the resistant strain is lower and, after auto-oxidation, a smaller amount of ROS is generated. The resistant parasite has upregulated ROS scavenging machinery and efficiently detoxifies the ROS generated. The synergistic effect of all these pathways may lead toward the decreased AmB sensitivity for the resistant parasite (Fig. 6). In contrast, the AmB sensitivity to the membrane is higher in the sensitive parasite due to the presence of membrane ergosterol (Table 2), and that is why the AmB uptake, as well as the intracellular AmB content, is higher and the

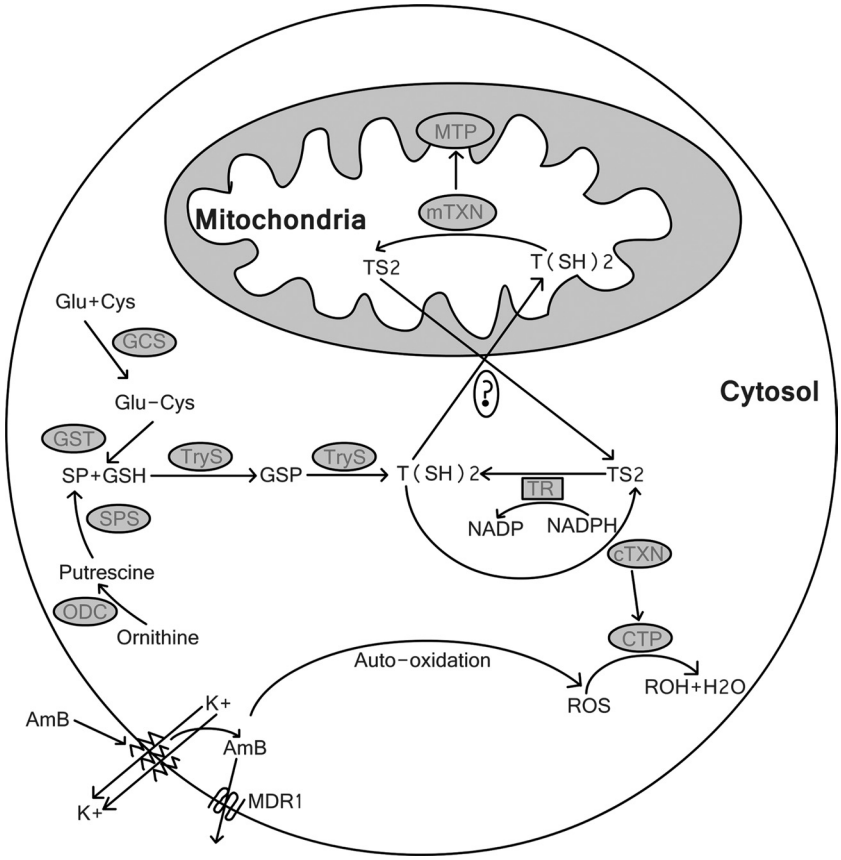

FIG 6 Hypothetical model showing intracellular events in conferring amphotericin B resistance. The model diagram illustrates the membrane composition, MDR1 (ABC transporters), and the tryparedoxin cascade of the thiol metabolic pathway, involved in various cellular actions in response to AmB and AmB-induced ROS. AmB binds with membrane ergosterol of sensitive *L. donovani* strains, causing membrane depolarization and leakage of ions like K^+ and leading to cell death. In contrast, AmB binding with the membrane in resistant strains is impaired due to an altered sterol profile (loss of function of the SCMT gene) of the membrane. A small amount of AmB may manage to be taken up into the resistant parasite, but some may also be effluxed out by the membrane-bound MDR1 and the remaining intracellular AmB auto-oxidizes and produces ROS. The toxic effect of this ROS may be nullified by the evolved tryparedoxin cascade of the thiol metabolic pathway. CTP of cytosol and MTP of mitochondria, terminal enzymes of the tryparedoxin cascade, may cleave the ROS. These cumulative effects of an altered membrane profile, evolved MDR1, and the tryparedoxin cascade may be responsible for making the *L. donovani* parasite resistant to AmB.

efflux of AmB is poor in the sensitive parasite. This, in turn, generates a larger amount of ROS after auto-oxidation of a larger amount of intracellular AmB. The ROS scavenging cascade is also not overexpressed in the sensitive parasite, and hence, the sensitive parasite probably undergoes an ROS-mediated killing when exposed to AmB (Fig. 6).

ACKNOWLEDGMENTS

This work was funded by a grant from the Indian Council of Medical Research (ICMR), Ministry of Health and Family Welfare, India.

We are thankful to Chetram Meena, Binod Yadav, Sohini Roy, and Debraj Saha for providing technical assistance for this study.

There was no conflict of interest.

REFERENCES

1. **Arana FE, et al.** 1998. Involvement of thiol metabolism in resistance to glucantime in *Leishmania tropica.* Biochem. Pharmacol. **56**:1201–1208.
2. **Baginski M, Czub J.** 2009. Amphotericin B and its new derivatives—mode of action. Curr. Drug Metab. **10**:459–469.
3. **Bloch KE.** 1983. Sterol structure and membrane function. CRC Crit. Rev. Biochem. **14**:47–92.
4. **Blum G, et al.** 2008. Potential basis for amphotericin B resistance in *Aspergillus terreus.* Antimicrob. Agents Chemother. **52**:1553–1555.
5. **Bolard J.** 1986. How do the polyene macrolide antibiotics affect the cellular membrane properties? Biochim. Biophys. Acta **864**:257–304.
6. **Boveris A, et al.** 1980. Deficient metabolic utilization of hydrogen peroxide in *Trypanosoma cruzi.* Biochem. J. **188**:643–648.
7. **Brajtburg J, Elberg S, Kobayashi GS, Medoff G.** 1986. Toxicity and induction of resistance to *Listeria monocytogenes* infection by amphotericin B in inbred strains of mice. Infect. Immun. **54**:303–307.
8. **Brajtburg J, Powderly WG, Kobayashi GS, Medoff G.** 1990. Amphotericin B: current understanding of mechanisms of action. Antimicrob. Agents Chemother. **34**:183–188.
9. **Brajtburg J, Powderly WG, Kobayashi GS, Medoff G.** 1990. Amphotericin B: delivery system. Antimicrob. Agents Chemother. **34**:381–384.
10. **Cai C, Zhu H, Chen J.** 2004. Overexpression of caveolin-1 increases plasma membrane fluidity and reduces P-glycoprotein function in Hs578T/Dox. Biochem. Biophys. Res. Commun. **320**:868–874.
11. **Castro H, et al.** 2002. Complementary antioxidant defense by cytoplasmic and mitochondrial peroxiredoxins in *Leishmania infantum.* Free Radic. Biol. Med. **33**:1552–1562.
12. **Croft SL, Sundar S, Fairlamb AH.** 2006. Drug resistance in leishmaniasis. Clin. Microbiol. Rev. **19**:111–126.
13. **Demel RA, de Kruyff B.** 1976. The function of sterols in membranes. Biochim. Biophys. Acta **457**:109–132.
14. **Dube A, Singh N, Sundar S, Singh N.** 2005. Refractoriness to the treatment of sodium stibogluconate in Indian kalaazar field isolates persists in in-vitro and in-vivo experimental models. Parasitol. Res. **96**:216–223.

15. **Dutcher JD, Gold W, Pagano JF, Vandepatte J.** September 1959. Amphotericin B, its production and its salts. US patent 2,908,611.
16. **Ellman GL.** 1959. Tissue sulfhydryl groups. Arch. Biochem. Biophys. **82**: 70–77.
17. **Fairlamb AH, Cerami A.** 1992. Metabolism and functions of trypanothione in the Kinetoplastida. Annu. Rev. Microbiol. **46**:695–729.
18. **Fairlamb AH, Blackburn P, Ulrich P, Chait BT, Cerami A.** 1985. Trypanothione: a novel bis (glutathionyl) spermidine cofactor for glutathione reductase in trypanosomatids. Science **227**:1485–1487.
19. **Flohé L, Hecht HJ, Steinert P.** 1999. Glutathione and trypanothione in parasitic hydroperoxide metabolism. Free Radic. Biol. Med. **27**:966–984.
20. **Fojo A, Akiyama S, Gottesman MM, Pastan I.** 1985. Reduced drug accumulation in multiply drug-resistant human KB carcinoma cell lines. Cancer Res. **45**:3002–3007.
21. **Galli G, Maroni S.** 1967. Mass spectrometric investigations of some unsaturated sterols biosynthetically related to cholesterol. Steroids **10**: 189–197.
22. **Goad LJ, Holtz GG, Jr, Beach DH.** 1984. Sterols of *Leishmania* species. Implications for biosynthesis. Mol. Biochem. Parasitol. **10**:161–170.
23. **Goad LJ, Holtz GG, Jr, Beach DH.** 1985. Sterols of ketoconazole inhibited *Leishmania mexicana mexicana* promastigotes. Mol. Biochem. Parasitol. **15**:257–279.
24. **Grondin K, Haimeur A, Mukhopadhyay R, Rosen BP, Ouellette M.** 1997. Co-amplification of the gamma-glutamylcysteine synthetase gene *gsh1* and of the ABC transporter gene *pgpA* in arsenite-resistant *Leishmania tarentolae.* EMBO J. **16**:3057–3065.
25. **Henderson DM, et al.** 1992. Multidrug resistance in *Leishmania donovani* is conferred by amplification of a gene homologous to the mammalian mdr1 gene. Mol. Cell. Biol. **12**:2855–2865.
26. **Higgins CF.** 1992. ABC transporters: from microorganisms to man. Annu. Rev. Cell Biol. **8**:67–113.
27. **HsuChen C-C, Feingold DS.** 1973. Polyene antibiotic action on lecithin liposomes: effect of cholesterol and fatty acyl chains. Biochem. Biophys. Res. Commun. **51**:972–978.
28. **Jha TK, Giri YN, Singh TK, Jha S.** 1995. Use of amphotericin B in drug-resistant cases of visceral leishmaniasis in north Bihar, India. Am. J. Trop. Med. Hyg. **52**:536–538.
29. **Kawato S, Kinoshita K, Ikegami A.** 1977. Dynamic structure of lipid bilayers studied by nanosecond fluorescence techniques. Biochemistry **16**: 2319–2324.
30. **Knights BA.** 1967. Identification of plant sterol using combined GLC/mass spectrometry. J. Gas Chromatogr. **5**:273–282.
31. **Krauth-Siegel RL, Bauer H, Schirmer RH.** 2005. Dithiol proteins as guardians of the intracellular redox milieu in parasites: old and new drug targets in trypanosomes and malaria-causing plasmodia. Angew. Chem. Int. Ed. Engl. **44**:690–715.
32. **Lamy-Freund MT, Ferreira VFN, Schreier S.** 1985. Mechanism of inactivation of the polyene antibiotic amphotericin B: evidence for radical formation in the process of autooxidation. J. Antibiot. (Tokyo) **38**: 753–757.
33. **Lemke A, Kiderlen AF, Kayser O.** 2005. Amphotericin B. Appl. Microbiol. Biotechnol. **68**:151–162.
34. **Lentz BR.** 1993. Use of fluorescent probes to monitor order and motions within liposome bilayers. Chem. Phys. Lipids **64**:99–116.
35. **Lentz BR, Barenholz Y, Thompson TE.** 1976. Fluorescence depolarization studies of phase transitions and fluidity in phospholipids bilayers. 1. Single component phosphatidylcholine liposomes. Biochemistry **15**: 4521–4528.
36. **Lin YC, Hsu JY, Chiang SC, Lee ST.** 2005. Distinct overexpression of cytosolic and mitochondrial tryparedoxin peroxidases results in preferential detoxification of different oxidants in arsenite-resistant *Leishmania amazonensis* with and without DNA amplification. Mol. Biochem. Parasitol. **142**:66–75.
37. **Massey IJ, Djerassi C.** 1979. Structural and stereochemical applications of mass spectrometry in the marine sterol field. Synthesis and electron impact induced mass spectral fragmentation of D24 and D24 (28)-3β-hydroxy-D5-sterols. J. Org. Chem. **44**:2448–2456.
38. **Mbongo N, Loiseau PM, Billion MA, Robert-Gero M.** 1998. Mechanism of amphotericin B resistance in *Leishmania donovani* promastigotes. Antimicrob. Agents Chemother. **42**:352–357.
39. **McGonigle S, Dalton JP, James ER.** 1998. Peroxidoxins: a new antioxidant family. Parasitol. Today **14**:139–145.
40. **Mendez S, Nell M, Alunda JM.** 1996. *Leishmania infantum*: infection of macrophages in vitro with promastigotes. Int. J. Parasitol. **26**:619–622.
41. **Moreira W, Leprohon P, Ouellette M.** 2011. Tolerance to drug-induced cell death favours the acquisition of multidrug resistance in Leishmania. Cell Death Dis. doi:10.1038/cddis.2011.83.
42. **Mukhopadhyay R, et al.** 1996. Trypanothione overproduction and resistance to antimonials and arsenicals in *Leishmania.* Proc. Natl. Acad. Sci. U. S. A. **93**:10383–10387.
43. **Neal RA, Van BJ, McCoy NG, Iwobi M.** 1989. Reversal of drug resistance in *Trypanosoma cruzi* and *Leishmania donovani* by verapamil. Trans. R. Soc. Trop. Med. Hyg. **83**:197–198.
44. **Nogoceke E, Gommel DU, Kiess M, Kalisz HM, Flohe L.** 1997. A unique cascade of oxidoreductases catalyses trypanothione mediated peroxide metabolism in *Crithidia fasciculate.* Biol. Chem. **378**:827–836.
45. **Ouellette M, et al.** 1998. ABC transporters in *Leishmania* and their role in drug resistance. Drug Resist. Updat. **1**:43–48.
46. **Pahissa A.** 1997. Amphotericin B. Lipid complex versus liposomes. Which, why, when? Enferm. Infecc. Microbiol. Clin. **15**:1–3.
47. **Perez-Victoria JM, Parodi-Talice A, Torres C, Gamarro F, Castanys S.** 2001. ABC transporters in the protozoan parasite *Leishmania.* Int. Microbiol. **4**:159–166.
48. **Pourshafie M, et al.** 2004. Cloning of *S*-adenosyl-L-methionine:C-24-Δ-sterolmethyltransferase (ERG6) from *Leishmania donovani* and characterization of mRNAs in wild-type and amphotericin B-resistant promastigotes. Antimicrob. Agents Chemother. **48**:2409–2414.
49. **Ritmeijer K, Dejenie A, Assefa Y.** 2006. A comparison of miltefosine and sodium stibogluconate for treatment of visceral leishmaniasis in an Ethiopian population with high prevalence of HIV infection. Clin. Infect. Dis. **43**:357–364.
50. **Seifert K, Croft SL.** 2006. In vitro and in vivo interactions between miltefosine and other antileishmanial drugs. Antimicrob. Agents Chemother. **50**:73–79.
51. **Sinha PK, et al.** 2006. Pre- & post-treatment evaluation of immunological features in Indian visceral leishmaniasis (VL) patients with HIV coinfection. Indian J. Med. Res. **123**:197–202.
52. **Sokol-Anderson M, et al.** 1988. Role of cell defense against oxidative damage in the resistance of *Candida albicans* to the killing effect of amphotericin B. Antimicrob. Agents Chemother. **32**:702–705.
53. **Srivastava P, Prajapati VK, Rai M, Sundar S.** 2011. Unusual case of resistance to amphotericin B in visceral leishmaniasis in a region in India where leishmaniasis is not endemic. J. Clin. Microbiol. **49**:3088–3091.
54. **Sundar S, Jha TK, Thakur CP, Sinha PK, Bhattacharya SK.** 2007. Injectable paromomycin for visceral leishmaniasis in India. N. Engl. J. Med. **356**:2571–2581.
55. **Tetaud E, et al.** 2001. Molecular characterisation of mitochondrial and cytosolic trypanothione-dependent tryparedoxin peroxidases in *Trypanosoma brucei.* Mol. Biochem. Parasitol. **116**:171–183.
56. **Urbina JA, Cohen BE, Perozo E, Cornivelli L.** 1987. Spin-labeled amphotericin B: synthesis, characterization, biological and spectroscopic properties. Biochim. Biophys. Acta **897**:467–473.
57. **World Health Organization.** 1998. The World Health Report. WHO, Geneva, Switzerland. http://www.who.int/whr/1998/en/whr98_en.pdf.